

Production rates of $D_s^+ D_s^-$ and $D\bar{D}$ molecules in B decays

Jia-Ming Xie,¹ Ming-Zhu Liu^{2,1,*} and Li-Sheng Geng^{3,1,4,5,†}

¹*School of Physics, Beihang University, Beijing 102206, China*

²*School of Space and Environment, Beihang University, Beijing 102206, China*

³*Peng Huanwu Collaborative Center for Research and Education, Beihang University, Beijing 100191, China*

⁴*Beijing Key Laboratory of Advanced Nuclear Materials and Physics, Beihang University, Beijing 102206, China*

⁵*School of Physics and Microelectronics, Zhengzhou University, Zhengzhou, Henan 450001, China*



(Received 11 August 2022; accepted 11 December 2022; published 5 January 2023)

Motivated by the recent discovery of a charmonium $X(3960)$ in B decays by the LHCb Collaboration, the likely existence of two bound/virtual states (denoted by $X_{s\bar{s}}$ and $X_{q\bar{q}}$) below the $D_s^+ D_s^-$ and $D\bar{D}$ mass thresholds has been reexamined recently. In this work, we employ the effective Lagrangian approach to calculate their production rates in B decays utilizing triangle diagrams. Our results show that the production yields of $B^+ \rightarrow X_{s\bar{s}} K^+$ and $B^+ \rightarrow X_{q\bar{q}} K^+$ are of the order of 10^{-4} , in agreement with the relevant experimental data, which indicates that, if the $D_s^+ D_s^-$ and $D\bar{D}$ bound states indeed exist, they can be detected in B decays. Moreover, we calculate the production rate of $B^+ \rightarrow X(3960) K^+$ assuming that $X(3960)$ is a resonant state of $D_s^+ D_s^-$ and find that it is also of the order of 10^{-4} but a bit smaller than that as a $D_s^+ D_s^-$ bound state.

DOI: [10.1103/PhysRevD.107.016003](https://doi.org/10.1103/PhysRevD.107.016003)

I. INTRODUCTION

In 2004, the Belle Collaboration observed a state around 3940 MeV in the $J/\psi\omega$ invariant mass distribution of the $B \rightarrow J/\psi\omega K$ decay [1], which was later confirmed by the BABAR Collaboration in the same process but the mass was determined to be 3915 MeV [2]. In 2009, the Belle Collaboration observed a state near 3915 MeV in the $\gamma\gamma \rightarrow J/\psi\omega$ reaction [3]. Later the BABAR Collaboration determined the quantum number of this state to be $J^{PC} = 0^{++}$ [4]. In 2020, the LHCb Collaboration observed a similar state $\chi_{c0}(3930)$ in the $D^+ D^-$ mass distribution of the $B^+ \rightarrow D^+ D^- K^+$ decay [5,6]. In the Review of Particle Physics (RPG) [7], all these states are referred to as $\chi_{c0}(3915)$ and viewed as a candidate for the $\chi_{c0}(2P)$ charmonium [8,9]. Very recently, the LHCb Collaboration reported a charmonium state named as $X(3960)$ with $J^{PC} = 0^{++}$ in the $D_s^+ D_s^-$ mass distribution of the $B^+ \rightarrow D_s^+ D_s^- K^+$ decay. Its mass and width are determined to be $m = 3955 \pm 6 \pm 11$ MeV and $\Gamma = 48 \pm 17 \pm 10$ MeV [10].

*zhengmz11@buaa.edu.cn

†lisheng.geng@buaa.edu.cn

Published by the American Physical Society under the terms of the [Creative Commons Attribution 4.0 International license](https://creativecommons.org/licenses/by/4.0/). Further distribution of this work must maintain attribution to the author(s) and the published article's title, journal citation, and DOI. Funded by SCOAP³.

Given that the mass of $X(3960)$ is very different from that of $\chi_{c0}(3915)$, they are not likely to be the same state. It is also difficult to interpret $X(3960)$ as a conventional charmonium because the mass of $\chi_{c0}(3P)$ (in the quark model) is around 4200 MeV [11,12]. In Ref. [13], M. Bayar *et al.* argued that in the chiral unitary approach there exist two states below the $D\bar{D}$ and $D_s^+ D_s^-$ thresholds, respectively, and the new $X(3960)$ can be understood as an enhancement in the $D_s^+ D_s^-$ mass distribution. In Ref. [14], Xin *et al.* interpreted $X(3960)$ as a $J^{PC} = 0^{++}$ $D_s^+ D_s^-$ molecule in the QCD sum rules approach. With a leading order contact range effective field theory Ji *et al.* showed that either a bound state or a virtual state below the $D_s^+ D_s^-$ mass threshold is needed to describe the $D_s^+ D_s^-$ mass distribution of the $B^+ \rightarrow D_s^+ D_s^- K^+$ decay [15].

The likely existence of molecules near the $D\bar{D}$ and $D_s^+ D_s^-$ mass thresholds has been studied in several approaches before the experimental discoveries. In Ref. [16], Prelovsek *et al.* performed lattice QCD simulations of coupled-channel $D\bar{D}$ and $D_s^+ D_s^-$ interactions and found the existence of two bound states near the $D\bar{D}$ and $D_s^+ D_s^-$ mass thresholds. In Ref. [17], Gamermann *et al.* obtained a $I(J^{PC}) = 0(0^{++})$ narrow resonance with a mass of 3719 MeV, which mainly couples to the $D\bar{D}$ and $D_s \bar{D}_s$ channels. In our previous works [18,19], we investigated the $D\bar{D}$ interaction in the one boson exchange (OBE) model and found that a large cutoff of $\Lambda = 1.415$ GeV is needed to generate a $D\bar{D}$ bound state. On the other hand, in

order to reproduce $X(3872)$ as a $D^*\bar{D}$ bound state in the OBE model, one only needs a cutoff of $\Lambda = 1.01$ GeV. From this, one concludes that the $D\bar{D}$ interaction is less attractive than the $D^*\bar{D}$ interaction, in agreement with several recent studies [20–22].

In Refs. [23,24], the authors described the $D\bar{D}$ mass distribution of $\gamma\gamma \rightarrow D\bar{D}$ and demonstrated the existence of a bound state near the $D\bar{D}$ mass threshold. In Ref. [25], considering the state $X(3720)$ mainly coupled to $D\bar{D}$, Dai *et al.* predicted the $D\bar{D}$ mass distribution of the $B^- \rightarrow D^0\bar{D}^0K^-$ process. In Ref. [26], assuming $\chi_{c0}(3915)$ as a $D_s^+D_s^-$ bound state, Li *et al.* estimated the branching ratio of the $B^+ \rightarrow \chi_{c0}(3915)K^+$ decay to be 6×10^{-4} . In this work, we assume that there exist two molecules near the $D\bar{D}$ and $D_s^+D_s^-$ mass thresholds, denoted as $X_{q\bar{q}}$ and $X_{s\bar{s}}$, and employ the effective Lagrangian approach to investigate their production rates in B decays via the triangle mechanism. Such an approach has been applied to study the production of P_c and P_{cs} in the $\Lambda_b \rightarrow J/\psi pK$ [27] and $\Xi_b \rightarrow J/\psi \Lambda K$ decays [28]. The production rates of $D\bar{D}$ and $D_s^+D_s^-$ molecules in B decays are helpful to probe the nature of $X(3960)$ as well as to understand the $D\bar{D}$ and $D_s^+D_s^-$ interactions.

This work is organized as follows. We introduce the triangle mechanism for the decays of $B^+ \rightarrow X_{s\bar{s}}K^+$ and $B^+ \rightarrow X_{q\bar{q}}K^+$ and the effective Lagrangian approach in Sec. II. Results and discussions are given in Sec. III, followed by a short summary in the last section.

II. THEORETICAL FORMALISM

The B decays are a good platform to study the weak interaction and exotic states [29–32]. In this work, we employ the triangle diagram to investigate the weak decays of $B^+ \rightarrow X_{q\bar{q}}K^+$ and $B^+ \rightarrow X_{s\bar{s}}K^+$. At the quark level, the decays of $B^+ \rightarrow D_s^+\bar{D}^{*0}$ and $B^+ \rightarrow D_s^{*+}\bar{D}^0$ can both proceed through the external W -emission mechanism shown in Fig. 1. Referring to the Review of Particle Physics [7], the absolute branching fractions of the decay modes $B^+ \rightarrow D_s^+\bar{D}^{*0}$ and $B^+ \rightarrow D_s^{*+}\bar{D}^0$ are $(8.2 \pm 1.7) \times 10^{-3}$ and $(7.6 \pm 1.6) \times 10^{-3}$, respectively, which are larger

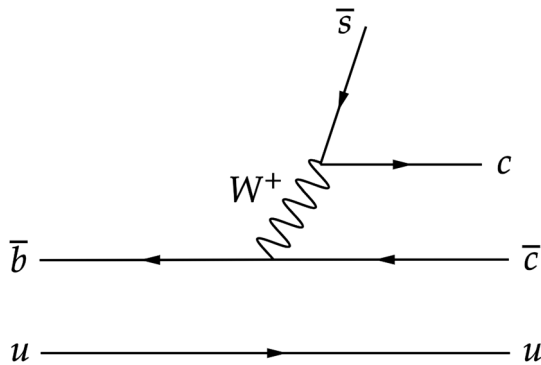


FIG. 1. External W -emission for $B^+ \rightarrow D_s^+\bar{D}^{*0}$ and $B^+ \rightarrow D_s^{*+}\bar{D}^0$.

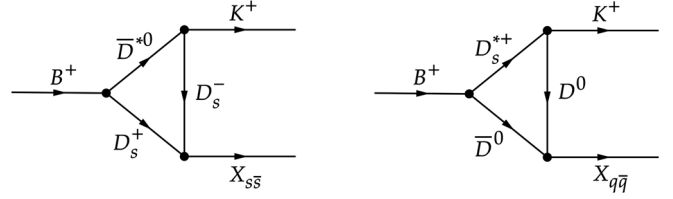


FIG. 2. Triangle diagrams accounting for the two B decays: (a) $B^+ \rightarrow D_s^+\bar{D}^{*0} \rightarrow X_{s\bar{s}}K^+$ and (b) $B^+ \rightarrow D_s^{*+}\bar{D}^0 \rightarrow X_{q\bar{q}}K^+$.

than those of the B meson decaying into a charmonium and a K^+ . Then, taking into account the interaction vertices of $\bar{D}^{*0} \rightarrow D_s^-K^+$ and $D_s^{*+} \rightarrow D^0K^+$, the $D_s^+D_s^-$ and \bar{D}^0D^0 molecules can be dynamically generated. We illustrate the decays of $B^+ \rightarrow X_{s\bar{s}}K^+$ and $B^+ \rightarrow X_{q\bar{q}}K^+$ at the hadron level via the triangle diagrams shown in Fig. 2. In the following, we introduce the effective Lagrangians relevant to the computation of the Feynman diagrams shown in Fig. 2.

The effective Hamiltonian describing the weak decays of $B^+ \rightarrow D_s^+\bar{D}^{*0}$ and $B^+ \rightarrow D_s^{*+}\bar{D}^0$ has the following form

$$\mathcal{H}_{\text{eff}} = \frac{G_F}{\sqrt{2}} V_{cb} V_{cs} [c_1^{\text{eff}} \mathcal{O}_1 + c_2^{\text{eff}} \mathcal{O}_2] + \text{H.c.}, \quad (1)$$

where G_F is the Fermi constant, V_{bc} and V_{cs} are the Cabibbo-Kobayashi-Maskawa (CKM) matrix elements, $c_{1,2}^{\text{eff}}$ are the effective Wilson coefficients, and \mathcal{O}_1 and \mathcal{O}_2 are the four-fermion operators of $(s\bar{c})_{V-A}(c\bar{b})_{V-A}$ and $(\bar{c}c)_{V-A}(s\bar{b})_{V-A}$ with $(\bar{q}q)_{V-A}$ standing for $\bar{q}\gamma_\mu(1-\gamma_5)q$ [33–35].

The amplitudes of $B^+ \rightarrow D_s^+\bar{D}^{*0}$ and $B^+ \rightarrow D_s^{*+}\bar{D}^0$ can be written as the products of two hadronic matrix elements [36,37]

$$\begin{aligned} \mathcal{A}(B^+ \rightarrow D_s^+\bar{D}^{*0}) &= \frac{G_F}{\sqrt{2}} V_{cb} V_{cs} a_1 \langle D_s^+ | (s\bar{c}) | 0 \rangle \\ &\quad \times \langle \bar{D}^{*0} | (c\bar{b}) | B^+ \rangle \end{aligned} \quad (2)$$

$$\begin{aligned} \mathcal{A}(B^+ \rightarrow D_s^{*+}\bar{D}^0) &= \frac{G_F}{\sqrt{2}} V_{cb} V_{cs} a'_1 \langle D_s^{*+} | (s\bar{c}) | 0 \rangle \\ &\quad \times \langle \bar{D}^0 | (c\bar{b}) | B^+ \rangle \end{aligned} \quad (3)$$

where $a_1^{(\prime)} = c_1^{\text{eff}} + c_2^{\text{eff}}/N_c$ with $N_c = 3$ the number of colors. It should be noted that a_1 and a'_1 can be obtained in the factorization approach [38].

The current matrix elements between a pseudoscalar meson or vector meson and the vacuum have the following form:

$$\begin{aligned} \langle D_s^+ | (s\bar{c}) | 0 \rangle &= g_{D_s} f_{D_s} p_{D_s}^\nu, \\ \langle D_s^{*+} | (s\bar{c}) | 0 \rangle &= m_{D_s^{*+}} f_{D_s^{*+}} \epsilon_\mu^*, \end{aligned} \quad (4)$$

where f_{D_s} and $f_{D_s^{*+}}$ are the decay constants for D_s and D_s^{*+} , respectively, and ϵ_μ^* is the polarization vector of D_s^{*+} .

The hadronic matrix elements can be parametrized in terms of a few form factors [39]

$$\langle \bar{D}^{*0} | (c\bar{b}) | B^+ \rangle = \epsilon_\alpha^* \left\{ -g^{\mu\alpha} (m_{\bar{D}^{*0}} + m_{B^+}) A_1(q^2) + P^\mu P^\alpha \frac{A_2(q^2)}{m_{\bar{D}^{*0}} + m_{B^+}} \right. \\ \left. + i\epsilon^{\mu\alpha\beta\gamma} P_\beta q_\gamma \frac{V(q^2)}{m_{\bar{D}^{*0}} + m_{B^+}} + q^\mu P^\alpha \left[\frac{m_{\bar{D}^{*0}} + m_{B^+}}{q^2} A_1(q^2) - \frac{m_{B^+} - m_{\bar{D}^{*0}}}{q^2} A_2(q^2) - \frac{2m_{\bar{D}^{*0}}}{q^2} A_0(q^2) \right] \right\}, \quad (5)$$

$$\langle \bar{D}^0 | (c\bar{b}) | B^+ \rangle = (p_{B^+} + p_{\bar{D}^0})^\mu F_{1D}(q^2) + q'^\mu F_{2D}(q^2), \quad (6)$$

where q and q' represent the momentum of D_s^+ and D_s^{*+} , respectively, and $P = (p_{B^+} + p_{\bar{D}^{*0}})$. The form factors of $F_{1,2D}(t)$, $A_0(t)$, $A_1(t)$, $A_2(t)$, and $V(t)$ with $t \equiv q^{(i)2}$ are parametrized as¹

$$X(t) = \frac{X(0)}{1 - a(t/m_B^2) + b(t^2/m_B^4)}, \quad (8)$$

which could well fit the transition form factors of $B \rightarrow \bar{D}^*$ as shown in Ref. [39].

The Lagrangian describing the interaction between the charmed mesons D_s , D^* and a kaon has the following form

$$\mathcal{L}_{D_s D^* K} = -ig_{D_s D^* K} (D_s \partial^\mu K D_\mu^{*\dagger} - D_\mu^* \partial^\mu K D_s^\dagger), \quad (9)$$

where $g_{D_s D^* K}$ is the coupling constant.

Assuming that $X_{s\bar{s}}$ and $X_{q\bar{q}}$ are dynamically generated by the $D_s^+ D_s^-$ and $\bar{D}D$ interactions, respectively, the relevant Lagrangians can be written as

$$\mathcal{L}_{X_{s\bar{s}} D_s^+ D_s^-}(x) = g_{X_{s\bar{s}} D_s^+ D_s^-} X_{s\bar{s}}(x) \int dy \Phi(y^2) \\ \times D_s^+ \left(x + \frac{1}{2}y \right) D_s^- \left(x - \frac{1}{2}y \right), \quad (10)$$

$$\mathcal{L}_{X_{q\bar{q}} \bar{D}D}(x) = g_{X_{q\bar{q}} \bar{D}D} X_{q\bar{q}}(x) \int dy \Phi(y^2) \\ \times \bar{D} \left(x + \frac{1}{2}y \right) D \left(x - \frac{1}{2}y \right). \quad (11)$$

As $X_{s\bar{s}}$ and $X_{q\bar{q}}$ are bound states of $D_s^+ D_s^-$ and $\bar{D}D$, we adopt the compositeness condition to estimate the couplings of $g_{X_{s\bar{s}} D_s^+ D_s^-}$ and $g_{X_{q\bar{q}} \bar{D}D}$. The correlation function $\Phi(y^2)$ is introduced to reflect the distribution of the two constituent hadrons in the molecule, which also renders the Feynman diagrams ultraviolet finite. Here we choose the Fourier transformation of the correlation function in form of a Gaussian function

$$\Phi(p^2) \doteq \text{Exp}(-p_E^2/\Lambda^2), \quad (12)$$

where Λ is a size parameter, which is expected to be around 1 GeV [44,45], and p_E is the Euclidean momentum. The couplings, $g_{X_{s\bar{s}} D_s^+ D_s^-}$ and $g_{X_{q\bar{q}} \bar{D}D}$, can be estimated by reproducing the binding energies of the $X_{s\bar{s}}$ and $X_{q\bar{q}}$ states via the compositeness condition [46–48]. The condition dictates that the coupling constant can be determined from the fact that the renormalization constant of the wave function of a composite particle should be zero. The compositeness condition can be estimated from the self energy

$$Z = 1 - \frac{d\Sigma(k_0^2)}{dk_0^2} \Big|_{k_0=m_X} = 0. \quad (13)$$

With the above relevant Lagrangians, one can easily compute the corresponding amplitudes of Fig. 2,

$$\mathcal{A}_a = g_{X_{s\bar{s}} D_s^+ D_s^-} \int \frac{d^4 q_3}{(2\pi)^4} \frac{i\mathcal{A}(B^+ \rightarrow D_s^+ \bar{D}^{*0}) \mathcal{A}(\bar{D}^{*0} \rightarrow D_s^- K^+)}{(q_1^2 - m_{\bar{D}^*}^2 + im_{\bar{D}^*} \Gamma_{\bar{D}^*})(q_2^2 - m_{D_s^+}^2)(q_3^2 - m_{D_s^-}^2)}, \quad (14)$$

¹The electric and magnetic distributions of hadrons in the low energy region, such as those of the nucleons, are often parametrized by dipole form factors of the following form:

$$G_{E,M}(q^2) = \frac{G_{E,M}(0)}{(1 + q^2/m^2)^2}, \quad (7)$$

which, however, need to be revised in the high energy region [40,41]. We note that the dipole form factors have also been adopted to describe the internal structure of baryons in lattice QCD simulations [42,43].

$$A_b = g_{X_{q\bar{q}}\bar{D}^0D^0} \int \frac{d^4q_3}{(2\pi)^4} \frac{i\mathcal{A}(B^+ \rightarrow D_s^{*+}\bar{D}^0)\mathcal{A}(D_s^{*+} \rightarrow D^0K^+)}{(q_1^2 - m_{D_s^{*+}}^2 + im_{D_s^{*+}}\Gamma_{D_s^{*+}})(q_2^2 - m_{\bar{D}^0}^2)(q_3^2 - m_{D^0}^2)}, \quad (15)$$

where q_1 , q_2 , and q_3 denote the momenta of \bar{D}^{*0} , D_s^+ , and D_s^- for Fig. 2(a) and D_s^{*+} , \bar{D}^0 , and D^0 for Fig. 2(b), and p_1 and p_2 represent the momenta of K^+ and $X_{s\bar{s}}(X_{q\bar{q}})$. The vertices of $X_{s\bar{s}}D_s^+D_s^-$ and $X_{q\bar{q}}\bar{D}^0D^0$ are parametrized as the couplings $g_{X_{s\bar{s}}D_s^+D_s^-}$ and $g_{X_{q\bar{q}}\bar{D}^0D^0}$,

respectively. The $\bar{D}^{*0} \rightarrow D_s^-K^+$ transition is expressed as $\mathcal{A}(\bar{D}^{*0} \rightarrow D_s^-K^+) = g_{\bar{D}^{*0}D_s^-K^+} p_1 \cdot \varepsilon(q_1)$, and the $D_s^{*+} \rightarrow D^0K^+$ transition is expressed as $\mathcal{A}(D_s^{*+} \rightarrow D^0K^+) = g_{D_s^{*+}D^0K^+} p_1 \cdot \varepsilon(q_1)$. The weak decay amplitudes of $B^+ \rightarrow D_s^+\bar{D}^{*0}$ and $B^+ \rightarrow D_s^+\bar{D}^0$ are written as

$$A(B \rightarrow D_s\bar{D}^*) = \frac{G_F}{\sqrt{2}} V_{cb} V_{cs} a_1 f_{D_s} \left\{ -q_2 \cdot \varepsilon(q_1) (m_{\bar{D}^{*0}} + m_{B^+}) A_1(q_2^2) + (k_0 + q_1) \cdot \varepsilon(q_1) q_2 \cdot (k_0 + q_1) \frac{A_2(q_2^2)}{m_{\bar{D}^{*0}} + m_{B^+}} \right. \\ \left. + (k_0 + q_1) \cdot \varepsilon(q_1) [(m_{\bar{D}^{*0}} + m_{B^+}) A_1(q_2^2) - (m_{B^+} - m_{\bar{D}^{*0}}) A_2(q_2^2) - 2m_{\bar{D}^{*0}} A_0(q_2^2)] \right\}, \\ A(B \rightarrow D_s^*\bar{D}) = \frac{G_F}{\sqrt{2}} V_{cb} V_{cs} a_1' f_{D_s^*} m_{D_s^*} \varepsilon(q_1) \cdot (k_0 + q_2) F_{1D}(q_1^2), \quad (16)$$

With the $B^+ \rightarrow X_{s\bar{s}}(X_{q\bar{q}})K^+$ amplitudes determined above, the corresponding partial decay widths can be finally written as

$$\Gamma = \frac{1}{2J+1} \frac{1}{8\pi} \frac{|\vec{p}|}{m_B^2} |\overline{\mathcal{M}}|^2, \quad (17)$$

where J is the total angular momentum of the initial B meson, the overline indicates the sum over the polarization vectors of final states, and $|\vec{p}|$ is the momentum of either final state in the rest frame of the B meson.

III. RESULTS AND DISCUSSIONS

The amplitudes of $B^+ \rightarrow D_s^+\bar{D}^{*0}$ and $B^+ \rightarrow D_s^+\bar{D}^0$ are obtained by the naive factorization approach as shown in Eq. (13). In this work, we take $G_F = 1.166 \times 10^{-5} \text{ GeV}^{-2}$, $V_{cb} = 0.041$, $V_{cs} = 0.987$, $f_{D_s} = 250 \text{ MeV}$, and $f_{D_s^*} = 272 \text{ MeV}$ as in Refs. [7,39,49–51]. For the form factors, we adopt those of the covariant light-front quark model, e.g., $(F_{1D}(0), a, b)^{B^+ \rightarrow \bar{D}^0} = (0.67, 1.22, 0.36)$, $(A_0(0), a, b)^{B^+ \rightarrow \bar{D}^{*0}} = (0.68, 1.21, 0.36)$, $(A_1(0), a, b)^{B^+ \rightarrow \bar{D}^{*0}} = (0.65, 0.60, 0.00)$, and $(A_2(0), a, b)^{B^+ \rightarrow \bar{D}^{*0}} = (0.61, 1.12, 0.31)$ [39]. Note that the terms containing $V(q^2)$ and $F_{2D}(q^2)$ do not contribute to the processes we study here. We tabulate the masses and quantum numbers of relevant particles in Table I. In terms of the branching ratios of $B^+ \rightarrow D_s^+\bar{D}^{*0}$ and $B^+ \rightarrow D_s^+\bar{D}^0$ we determine $a_1 = 0.93$ and $a_1' = 0.81$, consistent with the estimates of Ref. [36]. The couplings of $g_{D_s^+\bar{D}^{*0}K^+}$ and $g_{D_s^+\bar{D}^0K^+}$ are determined by the SU(3)-flavor symmetry, e.g., $g_{D_s^+\bar{D}^{*0}K^+} = g_{D_s^+\bar{D}^0K^+} = \sqrt{2}g_{\bar{D}^{*0}\bar{D}^0\pi^0}$, where $g_{\bar{D}^{*0}\bar{D}^0\pi^0} = 11.7$ is obtained from the decay width of $D^{*0} \rightarrow D^0\pi^0$ [7]. The couplings of $g_{X_{s\bar{s}}D_s^+D_s^-}$

and $g_{X_{q\bar{q}}\bar{D}^0D^0}$ depend on whether the $X_{s\bar{s}}$ and $X_{q\bar{q}}$ states are below or above the mass thresholds of $D_s^+D_s^-$ and $\bar{D}D$, which will be specified below.

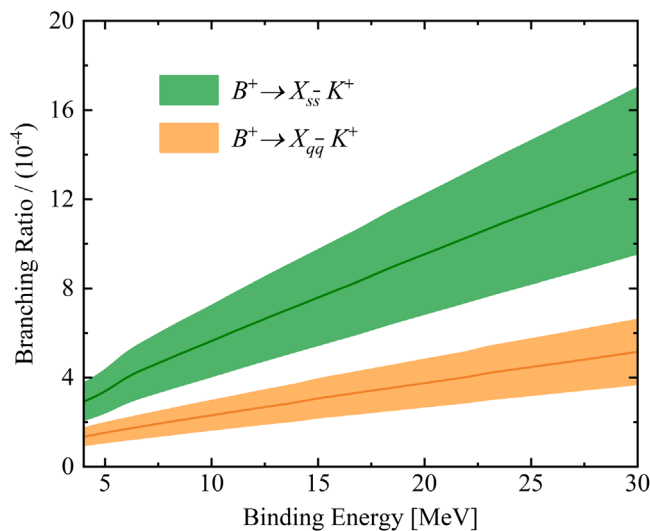
It is necessary to analyze the uncertainties of our results, which mainly come from the coupling constants needed to evaluate the triangle diagrams. In the weak interaction vertex, the uncertainties for the parameters $X(0)$, a and b of the transition form factors estimated in Ref. [39] are quite small and can be neglected. On the other hand, the uncertainties in the experimental branching ratios of $B \rightarrow \bar{D}^0D_s^{*+}/\bar{D}^{*0}D_s^+$ can propagate to the parameters a_1 (a_1') and lead to about 10% uncertainties for them, i.e., $a_1 = 0.93_{-0.10}^{+0.09}$ and $a_1' = 0.81_{-0.09}^{+0.08}$. For the scattering vertices $\bar{D}^{(*)}D_s^{(*)}K$, the couplings $g_{\bar{D}^{(*)}D_s^{(*)}K}$ are derived via SU(3)-flavor symmetry. Since SU(3)-flavor symmetry is broken at the level of 19% [52,53], we attribute an uncertainty of 19% to the $g_{\bar{D}^{(*)}D_s^{(*)}K}$ couplings. For the couplings $g_{X_{q\bar{q}}D\bar{D}}$ and $g_{X_{s\bar{s}}D_s^+D_s^-}$, we take a 10% uncertainty.² In terms of the average of the three uncertainties mentioned above, we arrive at an uncertainty of $\delta = 13\%$ for the couplings characterizing the triangle diagrams. Following Ref. [56], we estimate the uncertainty for the branching ratios in the following way $\Gamma = \Gamma(1 + \delta)^2$. As a result, the calculated branching ratios have an uncertainty of 28%.

²Following Refs. [54,55], we vary the cutoff from 1 GeV to 2 GeV, and the couplings $g_{X_{q\bar{q}}D\bar{D}}$ and $g_{X_{s\bar{s}}D_s^+D_s^-}$ decrease by approximately 10%. Similarly, with the cutoff $\Lambda = 2 \text{ GeV}$ and the contact potentials $C_a = -5.25 \text{ GeV}^{-2}$ and $C_b = -42.05 \text{ GeV}^{-4}$, we obtain the coupling $g_{X_{s\bar{s}}D_s^+D_s^-} = 8.69 \text{ GeV}$. Compared with the couplings obtained with the cutoff $\Lambda = 1 \text{ GeV}$ (as shown later), we find that the coupling $g_{X_{s\bar{s}}D_s^+D_s^-}$ increases by about 10%.

TABLE I. Masses and quantum numbers of mesons relevant to the present work [7].

Meson	$I(J^P)$	M (MeV)	Meson	$I(J^P)$	M (MeV)
B^+	$\frac{1}{2}(0^-)$	5279.34	K^+	$\frac{1}{2}(0^-)$	493.677
D^0	$\frac{1}{2}(0^-)$	1864.84	D^+	$\frac{1}{2}(0^-)$	1869.66
D^{*0}	$\frac{1}{2}(1^-)$	2006.85	D^{*+}	$\frac{1}{2}(1^-)$	2010.26
D_s^+	$0(0^-)$	1968.34	D_s^{*+}	$0(1^-)$	2112.2

If $X_{s\bar{s}}$ and $X_{q\bar{q}}$ are bound states, the coupling of $g_{X_{s\bar{s}}D_s^+D_s^-}$ and $g_{X_{q\bar{q}}\bar{D}^0D^0}$ can be estimated by the compositeness condition [45]. According to Refs. [13,15,16,25,26], we assume that $X_{s\bar{s}}$ and $X_{q\bar{q}}$ are located below the mass thresholds of $D_s^+D_s^-$ and $\bar{D}D$ respectively by 4 MeV to 30 MeV. For the $D_s^+D_s^-$ state, the coupling of $g_{X_{s\bar{s}}D_s^+D_s^-}$ is found to range from 9.41 GeV to 20.09 GeV, and the corresponding branching ratios of $B^+ \rightarrow X_{s\bar{s}}K^+$ varies from $(2.9 \pm 0.8) \times 10^{-4}$ to $(13.3 \pm 3.7) \times 10^{-4}$ as shown in Fig. 3. In Ref. [26], the authors assumed $\chi_{c0}(3915)$ as a $D_s^+D_s^-$ bound state and estimated the branching ratio of $B^+ \rightarrow \chi_{c0}(3915)K^+ = 6 \times 10^{-4}$, which agrees with our result $[(9.0 \pm 2.5) \times 10^{-4}]$ for a binding energy of $B = 20$ MeV approximately. Referring to the Review of Particle Physics [7], the upper limit of the branching ratio of $B^+ \rightarrow \chi_{c0}(3915)K^+$ is 2.8×10^{-4} , which is smaller than (but consistent with) our result. One should note that a shallow bound state below the $D_s^+D_s^-$ mass threshold is predicted in two recent works with a binding energy of only several MeV [13,15]. Obviously, the production ratio of such a shallow state in the $B^+ \rightarrow X_{s\bar{s}}K^+$ decay should be smaller than that of a deeply bound state, e.g., $\chi_{c0}(3915)$ treated as a $D_s^+D_s^-$ bound state, but should be of the same order as shown in Fig. 3. Therefore, our results indicate that


 FIG. 3. Branching ratios of $B^+ \rightarrow X_{s\bar{s}}K^+$ and $B^+ \rightarrow X_{q\bar{q}}K^+$ as functions of the binding energies of $D_s^+D_s^-$ and $\bar{D}D$ bound states.

the branching ratio of $B^+ \rightarrow X_{s\bar{s}}K^+$ is of the order of 10^{-4} if $X_{s\bar{s}}$ is a bound state of $D_s^+D_s^-$.

For the $\bar{D}D$ bound state, we determine the coupling of $g_{X_{q\bar{q}}\bar{D}D}$ as 9.62–19.38 GeV. The coupling of $g_{X_{q\bar{q}}\bar{D}^0D^0}$ is further determined by the isospin symmetry, i.e., $g_{X_{q\bar{q}}\bar{D}^0D^0} = \frac{1}{\sqrt{2}}g_{X_{q\bar{q}}\bar{D}D}$. With the couplings so obtained we calculate the branching ratio of $B^+ \rightarrow X_{q\bar{q}}K^+$, which turns out to be in the range of $(1.3 \pm 0.4 \sim 5.2 \pm 1.5) \times 10^{-4}$ as shown in Fig. 3. We note that the only allowed strong decay mode of a $\bar{D}D$ isoscalar molecule is $\eta_c\eta$, which implies that the branching ratio of $B^+ \rightarrow (X_{q\bar{q}} \rightarrow \eta_c\eta)K^+$ is 10^{-4} , which agrees well with the upper limit of the branching ratio of $B^+ \rightarrow \eta_c\eta K^+$, 2.2×10^{-4} [7]. Therefore, our result indicates that the $\bar{D}D$ bound state can be detected in the $\eta_c\eta$ mass distribution of the $B^+ \rightarrow \eta_c\eta K^+$ decay.

At last, we study the scenario where $X_{s\bar{s}}$ is a resonant state of $D_s^+D_s^-$, which can be identified as the $X(3960)$ state recently discovered by the LHCb Collaboration. Here we assume that $X(3960)$ is dynamically generated by the $D_s^+D_s^-$ interaction. With a contact potential of the form $C_a + C_b q^2$, one can reproduce the mass and width of $X(3960)$ by solving the Lippmann-Schwinger equation [57], and then obtain the $X(3960)$ coupling to $D_s^+D_s^-$ from the residues of the pole [58], where C_a and C_b are two low energy constants, and q is the momentum of D_s^\pm in the center-of-mass system of the $D_s^+D_s^-$ pair. With the experimental mass and width of $X(3960)$ as input, we obtain $C_a = -5.15 \text{ GeV}^{-2}$ and $C_b = -148.55 \text{ GeV}^{-4}$ for a cutoff of $\Lambda = 1 \text{ GeV}$, and then determine the coupling $g_{X_{s\bar{s}}D_s^+D_s^-} = 7.87 \text{ GeV}$. With the so-determined coupling we calculate the branching ratio of $B^+ \rightarrow X_{s\bar{s}}K^+$ and obtain $(1.9 \pm 0.5) \times 10^{-4}$.

IV. SUMMARY AND DISCUSSION

The recently discovered $X(3960)$ by the LHCb Collaboration motivated us to study the $D_s^+D_s^-$ and $\bar{D}D$ molecules predicted in a number of recent works. In this work, we assumed that there exist two bound states below the mass thresholds of $D_s^+D_s^-$ and $\bar{D}D$, respectively, and studied their production in the B decays via the triangle mechanism. In such a mechanism, B^+ first weakly decays into $D_s^+\bar{D}^{*0}$ and $D_s^{*+}\bar{D}^0$, the \bar{D}^{*0}/D_s^{*+} decays into D_s^-/D^0 plus a kaon, and then the final state $D_s^+D_s^-$ and \bar{D}^0D^0 interactions dynamically generate the $X_{s\bar{s}}$ and $X_{q\bar{q}}$ molecules. As for the bound states, we employed the compositeness condition approach to determine their couplings to their constituents. The resonant state of $D_s^+D_s^-$ is dynamically generated in the single-channel approximation, and the corresponding coupling is determined from the residues of the pole.

We employed the effective Lagrangian approach to calculate the branching ratios of $B^+ \rightarrow X_{s\bar{s}}K^+$ and $B^+ \rightarrow X_{q\bar{q}}K^+$ assuming that $X_{s\bar{s}}$ and $X_{q\bar{q}}$ are bound states and

TABLE II. Branching ratios of $B \rightarrow X_{s\bar{s}/q\bar{q}}/X(3960)K^+$ where $X_{s\bar{s}/q\bar{q}}$ is a bound state of $D_s^+D_s^-$ or $\bar{D}D$.

Decay modes	Our results	Exp [7]
$B^+ \rightarrow X_{s\bar{s}}K^+$	$(2.1 \sim 17.0) \times 10^{-4}$	$\text{Br}(B^+ \rightarrow \chi_{c0}(3915)K^+) < 2.8 \times 10^{-4}$
$B^+ \rightarrow (X_{q\bar{q}} \rightarrow \eta_c\eta)K^+$	$(0.9 \sim 6.7) \times 10^{-4}$	$\text{Br}(B^+ \rightarrow \eta_c\eta K^+) < 2.2 \times 10^{-4}$
$B^+ \rightarrow X(3960)K^+$	$< 2.4 \times 10^{-4}$...

found that both of them are of the order of 10^{-4} . Our results indicate that such bound states of $\bar{D}D$ and $D_s^+D_s^-$ (if exist) have large production rates in the B decays since they account for a large portion of the relevant experimental data as shown in Table II. We note that the $\bar{D}D$ bound state is likely to be detected in the $\eta_c\eta$ mass distribution of the $B^+ \rightarrow \eta_c\eta K^+$ decay since the $\bar{D}D$ bound state only decays into $\eta_c\eta$, while the $D_s^+D_s^-$ bound state has more decay modes, e.g., $B^+ \rightarrow \bar{D}DK^+$, $B^+ \rightarrow \eta_c\eta K^+$, and $B^+ \rightarrow J/\psi\omega K^+$. At last, assuming that the $X(3960)$ state is dynamically generated by the $D_s^+D_s^-$ single-channel interaction, we obtained the branching ratio of

$B^+ \rightarrow X(3960)K^+ = (1.9 \pm 0.5) \times 10^{-4}$, which can help elucidate the nature of $X(3960)$.

ACKNOWLEDGMENTS

This work is supported in part by the National Natural Science Foundation of China under Grants No. 11975041, No. 11735003, and No. 11961141004. M.-Z. L. acknowledges support from the National Natural Science Foundation of China under Grant No. 12105007 and China Postdoctoral Science Foundation under Grants No. 2022M710317, and No. 2022T150036.

-
- [1] K. Abe *et al.* (Belle Collaboration), *Phys. Rev. Lett.* **94**, 182002 (2005).
- [2] B. Aubert *et al.* (BABAR Collaboration), *Phys. Rev. Lett.* **101**, 082001 (2008).
- [3] S. Uehara *et al.* (Belle Collaboration), *Phys. Rev. Lett.* **104**, 092001 (2010).
- [4] J. P. Lees *et al.* (BABAR Collaboration), *Phys. Rev. D* **86**, 072002 (2012).
- [5] R. Aaij *et al.* (LHCb Collaboration), *Phys. Rev. D* **102**, 112003 (2020).
- [6] R. Aaij *et al.* (LHCb Collaboration), *Phys. Rev. Lett.* **125**, 242001 (2020).
- [7] P. A. Zyla *et al.* (Particle Data Group), *Prog. Theor. Exp. Phys.* **2020**, 083C01 (2020).
- [8] M.-X. Duan, S.-Q. Luo, X. Liu, and T. Matsuki, *Phys. Rev. D* **101**, 054029 (2020).
- [9] M.-X. Duan, J.-Z. Wang, Y.-S. Li, and X. Liu, *Phys. Rev. D* **104**, 034035 (2021).
- [10] LHCb Collaboration, arXiv:2211.05034; arXiv:2210.15153.
- [11] T. Barnes, S. Godfrey, and E. S. Swanson, *Phys. Rev. D* **72**, 054026 (2005).
- [12] B.-Q. Li and K.-T. Chao, *Phys. Rev. D* **79**, 094004 (2009).
- [13] M. Bayar, A. Feijoo, and E. Oset, arXiv:2207.08490.
- [14] Q. Xin, Z.-G. Wang, and X.-S. Yang, *AAPPS Bull.* **32**, 37 (2022).
- [15] T. Ji, X.-K. Dong, M. Albaladejo, M.-L. Du, F.-K. Guo, and J. Nieves, *Phys. Rev. D* **106**, 094002 (2022).
- [16] S. Prelovsek, S. Collins, D. Mohler, M. Padmanath, and S. Piemonte, *J. High Energy Phys.* **06** (2021) 035.
- [17] D. Gamermann, E. Oset, D. Strottman, and M. J. Vicente Vacas, *Phys. Rev. D* **76**, 074016 (2007).
- [18] M.-Z. Liu, T.-W. Wu, M. Pavon Valderrama, J.-J. Xie, and L.-S. Geng, *Phys. Rev. D* **99**, 094018 (2019).
- [19] T.-W. Wu, M.-Z. Liu, and L.-S. Geng, *Phys. Rev. D* **103**, L031501 (2021).
- [20] M.-Z. Liu and L.-S. Geng, *Eur. Phys. J. C* **81**, 179 (2021).
- [21] X.-K. Dong, F.-K. Guo, and B.-S. Zou, *Prog. Phys.* **41**, 65 (2021).
- [22] F.-Z. Peng, M. Sánchez Sánchez, M.-J. Yan, and M. Pavon Valderrama, *Phys. Rev. D* **105**, 034028 (2022).
- [23] E. Wang, H.-S. Li, W.-H. Liang, and E. Oset, *Phys. Rev. D* **103**, 054008 (2021).
- [24] O. Deineka, I. Danilkin, and M. Vanderhaeghen, *Phys. Lett. B* **827**, 136982 (2022).
- [25] L. R. Dai, J.-J. Xie, and E. Oset, *Eur. Phys. J. C* **76**, 121 (2016).
- [26] X. Li and M. B. Voloshin, *Phys. Rev. D* **91**, 114014 (2015).
- [27] Q. Wu and D.-Y. Chen, *Phys. Rev. D* **100**, 114002 (2019).
- [28] J.-X. Lu, M.-Z. Liu, R.-X. Shi, and L.-S. Geng, *Phys. Rev. D* **104**, 034022 (2021).
- [29] H.-Y. Cheng, C.-K. Chua, and A. Soni, *Phys. Rev. D* **71**, 014030 (2005).
- [30] H.-Y. Cheng and K.-C. Yang, *Phys. Rev. D* **78**, 094001 (2008); **79**, 039903(E) (2009).
- [31] H.-X. Chen, *Phys. Rev. D* **105**, 094003 (2022).
- [32] F.-L. Wang, X.-D. Yang, R. Chen, and X. Liu, *Phys. Rev. D* **104**, 094010 (2021).
- [33] A. J. Buras, Weak Hamiltonian, CP violation and rare decays, arXiv:hep-ph/9806471.
- [34] C. Q. Geng, Y. K. Hsiao, Y.-H. Lin, and L.-L. Liu, *Phys. Lett. B* **776**, 265 (2018).

- [35] J.-J. Han, H.-Y. Jiang, W. Liu, Z.-J. Xiao, and F.-S. Yu, *Chin. Phys. C* **45**, 053105 (2021).
- [36] A. Ali, G. Kramer, and C.-D. Lu, *Phys. Rev. D* **58**, 094009 (1998).
- [37] Q. Qin, H.-n. Li, C.-D. Lü, and F.-S. Yu, *Phys. Rev. D* **89**, 054006 (2014).
- [38] M. Bauer, B. Stech, and M. Wirbel, *Z. Phys. C* **34**, 103 (1987).
- [39] R. C. Verma, *J. Phys. G* **39**, 025005 (2012).
- [40] J. Arrington, C. D. Roberts, and J. M. Zanotti, *J. Phys. G* **34**, S23 (2007).
- [41] V. Punjabi, C. F. Perdrisat, M. K. Jones, E. J. Brash, and C. E. Carlson, *Eur. Phys. J. A* **51**, 79 (2015).
- [42] S. Collins *et al.*, *Phys. Rev. D* **84**, 074507 (2011).
- [43] K. U. Can, G. Erkol, B. Isildak, M. Oka, and T. T. Takahashi, *J. High Energy Phys.* **05** (2014) 125.
- [44] X.-Z. Ling, J.-X. Lu, M.-Z. Liu, and L.-S. Geng, *Phys. Rev. D* **104**, 074022 (2021).
- [45] X.-Z. Ling, M.-Z. Liu, L.-S. Geng, E. Wang, and J.-J. Xie, *Phys. Lett. B* **826**, 136897 (2022).
- [46] S. Weinberg, *Phys. Rev.* **130**, 776 (1963).
- [47] A. Salam, *Nuovo Cimento* **25**, 224 (1962).
- [48] K. Hayashi, M. Hirayama, T. Muta, N. Seto, and T. Shirafuji, *Fortschr. Phys.* **15**, 625 (1967).
- [49] S. Aoki *et al.* (Flavour Lattice Averaging Group), *Eur. Phys. J. C* **80**, 113 (2020).
- [50] G. C. Donald, C. T. H. Davies, R. J. Dowdall, E. Follana, K. Hornbostel, J. Koponen, G. P. Lepage, and C. McNeile, *Phys. Rev. D* **86**, 094501 (2012).
- [51] Y. Li, P. Maris, and J. P. Vary, *Phys. Rev. D* **96**, 016022 (2017).
- [52] S. Dürr *et al.*, *Phys. Rev. D* **95**, 054513 (2017).
- [53] N. Miller *et al.*, *Phys. Rev. D* **102**, 034507 (2020).
- [54] A. Faessler, T. Gutsche, V. E. Lyubovitskij, and Y.-L. Ma, *Phys. Rev. D* **76**, 014005 (2007).
- [55] A. Faessler, T. Gutsche, S. Kovalenko, and V. E. Lyubovitskij, *Phys. Rev. D* **76**, 014003 (2007).
- [56] X.-Z. Ling, M.-Z. Liu, and L.-S. Geng, *Eur. Phys. J. C* **81**, 1090 (2021).
- [57] Q.-Y. Zhai, M.-Z. Liu, J.-X. Lu, and L.-S. Geng, *Phys. Rev. D* **106**, 034026 (2022).
- [58] J.-M. Xie, X.-Z. Ling, M.-Z. Liu, and L.-S. Geng, *Eur. Phys. J. C* **82**, 1061 (2022).